Progress in Oceanography 86 (2010) 380–395

Contents lists available at ScienceDirect

Progress in Oceanography

journal homepage: www.elsevier.com/locate/pocean

On the natural oscillations of Monterey Bay: Observations, modeling, and origins

Laurence C. Breaker [a,*], Yu-heng Tseng [b], Xiaochun Wang [c]

[a] Moss Landing Marine Laboratories, Moss Landing, CA 93950, United States
[b] Department of Atmospheric Sciences, National Taiwan University, Taipei, Taiwan
[c] Joint Institute for Regional Earth System Science and Engineering, University of California at Los Angeles, Los Angeles, CA 90095, United States

ARTICLE INFO

Article history:
Received 28 July 2009
Received in revised form 2 June 2010
Accepted 8 June 2010
Available online 16 June 2010

ABSTRACT

Observations of the natural oscillations of Monterey Bay have revealed periods that range from several minutes to almost one hour. These oscillations can be excited by winter storm events, and historical data show that they were also excited by tsunamis produced by the 1989 Loma Prieta Earthquake and the 1964 Great Alaskan Earthquake. However, these oscillations also tend to be continuous in nature although low in amplitude. The four lowest frequency oscillations have periods of approximately 55, 36, 27, and 22 min. The 55-min period corresponds to the first longitudinal mode of oscillation, and the 36-min period, to the first transverse mode. Numerical simulations are employed to examine the oscillating characteristics of the bay and to help ascertain their origin. The model results are consistent with earlier studies, suggesting that Monterey Submarine Canyon divides the bay into two separate oscillating basins, although water level and pressure data indicate that at least for the four lowest frequencies, these oscillations tend to be bay-wide. Spatial patterns extracted from model-generated power spectra at the four lowest frequencies show good agreement with the modal patterns predicted by Wilson et al. (1965).

Impulsively generated seiche oscillations should be subject to relatively strong damping and consequently decay within several cycles. Thus, it is not clear why the oscillations tend to be continuous, since the natural oscillations that are observed in most basins are transient, due to the transient nature of the forcing. Model simulations further indicate that both wind and tidal forcing contribute to the oscillations. Several mechanisms that could be responsible for the natural oscillations of Monterey Bay on a continuous basis were considered but it is not clear which, if any, of these mechanisms is ultimately responsible for exciting them. However, if the source of their excitation is wide-ranging or global, then they are likely to occur elsewhere around the world as well.

1. Introduction

Any water body experiences free or natural oscillations that are referred to as normal modes (e.g., Kowalik and Murty, 1993), and different mechanisms can excite these normal modes. Their frequencies can be determined entirely from a knowledge of the geometry of the water body and the water depth. These natural oscillations are not influenced by the nature of the forcing (e.g., Sobey, 2006). The study of normal modes has a long and distinguished history going back to the work of LaPlace (1775) and Hough (1898). Normal modes that occur in enclosed and semi-enclosed bodies of water are often referred to as seiches.

More specifically, seiches are standing waves that occur in enclosed or semi-enclosed basins such as lakes, gulfs, bays and harbors. Neglecting the effects of earth rotation, for a rectangular basin of constant depth, H, horizontal dimension, L, and g, the acceleration of gravity, the period of the oscillation, T, is given by

$$T = 2L/\sqrt{gH}. \quad (1)$$

T represents the time for a progressive wave to propagate from one end of the basin to the other, and back. This relation is often called Merian's formula. For a semi-circular basin and a semi-parabolic bottom, oriented in the offshore direction, the fundamental period of free oscillation is given by

$$T = 2.22L/\sqrt{gH_1}, \quad (2)$$

where H_1 represents the depth at the deepest point on the parabola (Wilson et al., 1965). This modified form of Merian's formula provides a much closer approximation to the configuration of Monterey Bay. In more complicated cases, where the configuration of the basin does not conform to a simple geometrical shape, a number of numerical approaches can be used to estimate the natural periods of oscillation including state-of-the-art hydrodynamic circulation models.

The description above does not take into account frictional effects. The viscosity of the fluid and bottom friction cause the amplitude of natural oscillations to decay rapidly, whereas the period of

* Corresponding author.
E-mail address: laurence.breaker@gmail.com (L.C. Breaker).

0079-6611/$ - see front matter © 2010 Elsevier Ltd. All rights reserved.
doi:10.1016/j.pocean.2010.06.001

the oscillations increases slightly. In most cases, these oscillations do not last for more than 5 or 6 cycles (Neumann and Pierson, 1966). The influence of friction on the period depends slightly on water depth, decreasing as depth increases (Defant, 1961).

In partially open basins such as bays and gulfs, waters within the basin must communicate with the waters outside. Thus, a nodal line exists across the entrance of these basins. According to Wilson (1972), the longest free oscillation of a bay must be identical with that of a basin consisting of two identical sections which are mirror images with respect to the opening which joins the two parts. For a bay of length, L, where L is now directed toward the mouth of the bay whose cross section is rectangular and whose depth is constant, the period associated with the longest free oscillation is given by

$$T = 4L/\sqrt{gH}, \tag{3}$$

where the modal period is the same as that given by (1) if L is replaced by $2L$. A correction may have to be applied for bays that have a wide entrance to the open sea where the width of the entrance is a significant fraction of the length of the bay. The magnitude of the correction increases as the ratio of the width of the bay to its length increases.

The effect of the earth's rotation on seiches has also been examined and depends on the size of the basin, increasing, as the basin size increases. Its effect, however, is small. For the Baltic Sea, for example, which is more than 100 times larger than Monterey Bay, the increase in period due to the earth's rotation was found to be less than 1% (Defant, 1961). In cases where the configuration of the lake or bay is complicated, the region of oscillation may not be adequately represented by a single mode. In such cases, the total oscillatory system may be split into separate parts. These parts, taken together, then form the complete oscillatory system for that basin.

In Hakodate Bay off the coast of Japan, a bay somewhat similar in configuration to Monterey Bay, Honda et al. (1908) found from tide gauge measurements that a principal seiche with a nodal line across the opening of the bay had periods that ranged from 45.5 to 57.7 min, and that there was a transverse seiche that had periods ranging from 21.9 to 24.6 min. As we will see, observations from tide and pressure gauges show similar variability in the measured periods associated with the primary modes of oscillation in Monterey Bay.

Seiches can be initiated by several factors including sudden changes in the wind and/or barometric pressure, and seismic disturbances. In the case of wind forcing, when it causes water to accumulate at one end of a basin, a sudden cessation of the wind can cause seiching to occur. Defant (1961) gives seven weather-related causes of oscillatory motions in lakes and bays and they are all impulsive in nature. In addition to the above, Wilson (1972) distinguishes between seiches that occur in lakes and bays, and those that are coastal in nature, where coastal seiches can excite natural oscillations within bays and harbors through the direct impression of wave energy at the entrances to such coastally-connected basins. Seiches can also be caused by seismic disturbances and tsunamis (e.g., Murty, 1977), ocean swell (e.g., Okihiro and Guza, 1996), edge waves (Lemon, 1975), and internal waves (Giese et al., 1990).

The natural oscillations of Monterey Bay or seiche modes have been examined on several occasions. In a comprehensive study on surging in Monterey Harbor, Wilson et al. (1965)[1] examined the oscillating characteristics of Monterey Bay using a hierarchy of increasingly sophisticated analytical and numerical techniques to estimate the expected periods of oscillation. They initially applied analytical methods of analysis to various simple geometrical shapes to approximate the oscillating modes of the bay.

Then WHK employed more sophisticated procedures based on numerical approximations to the one-dimensional equation of motion and continuity to obtain more accurate results. In describing the oscillating characteristics of the bay, the primary mode of oscillation that was oriented essentially in the north–south direction was referred to as longitudinal, and the mode of oscillation oriented along the axis of Monterey Submarine Canyon (MSC) in essentially the east–west direction, where a nodal line exists across the entrance, was referred to as transverse. This nodal line was assumed to extend from Pt. Piños on the Monterey Peninsula, to Santa Cruz Point, at the north end of the bay (Fig. 1). Based on Eqs. (1) and (3), it is clear that the longest natural periods of oscillation occur in the longitudinal direction since the bay is approximately twice as long in this direction (~40 km) as it is in the transverse direction (~20 km). Analytic and numerical procedures were employed to extract the one, two, and three-dimensional modes of oscillation yielding somewhat different results, and many higher modes. The three-dimensional numerical analyses were only considered reliable for the lowest modes of oscillation because of the uncertainty of whether or not the nodal condition across the mouth of the bay could be sustained for the higher modes. The predicted periods, T_n, based on three-dimensional modes of oscillation for $n = 1$–8, were 44.2, 29.6, 28.2, 23.3, 21.6, 20.4, 19.4, and 18.7 min. The three-dimensional modes revealed that the MSC has a profound effect on the oscillating system (Fig. 1).

Water level measurements were also acquired during the study and so it was possible to compare the observations with the modes of oscillation that were predicted. Frequency analysis of the water level data yielded periods ranging from less than 5 min, to 66 min. The canyon essentially separates the bay into two semi-independent halves with only weak coupling between them. The oscillating regime of Monterey Harbor was also examined as a separate problem, yielding observed and predicted periods of oscillation in the range of 1–2 min to 13.3 min. They concluded that reasonable agreement was found between the measurements and the predicted modes of oscillation. However,

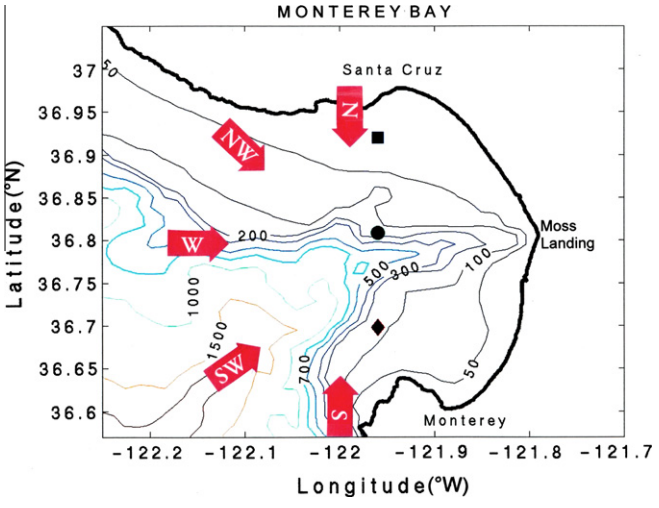

Fig. 1. The Monterey Bay region with bathymetric contours (meters). The five directions from which impulsive wind forcing is applied in the MBARM model are shown by red arrows. The black square, circle, and diamond show the locations where results from the model simulations were obtained (Fig. 7). (For interpretation of the references to colour in this figure legend, the reader is referred to the web version of this article.)

[1] From here on, we refer to Wilson et al. (1965) as WHK.

it was acknowledged that the nodal condition that was assumed to exist between Pt. Piños and Santa Cruz Point was open to question. It was concluded that long-period surface waves due to low-frequency oscillations in the atmosphere from extratropical disturbances, and not surf beat, was most likely responsible for producing the surge phenomenon in Monterey Harbor that lead to seiching. As we shall see, there are other explanations for the occurrence of seiche oscillations in Monterey Bay. Finally, they acknowledged that the nature of the forcing for the natural modes of oscillation for Monterey Bay is not well understood.

O'Connor (1964) examined sea level anomalies from tide gauge measurements in Monterey Harbor for a 6-month period and found that the largest anomalies were due to the vigorous sea breeze circulation in Monterey Bay. Sea level departures as large as 27 cm were attributed to the effects of the sea breeze. Raines (1967) analyzed 3 years of tidal records from Monterey Harbor and found oscillations with periods in the range of 1.5–2.0 min, and from 19 to 39 min. He indicated that the longer period oscillations could also be due to seiching within the bay. Robinson (1969), based on spectral analysis of water levels from Monterey Harbor and the Santa Cruz wharf, found that seiching contributed to the long-wave activity he observed. He also found that seiche oscillations have similar amplitudes at opposite ends of the bay, i.e., at Monterey and Santa Cruz. Based on auto- and cross-spectral analyses of water levels at Monterey Harbor and the Santa Cruz wharf, Lynch (1970) reported oscillations with periods of approximately 55, 36, and 27 min. These oscillations were attributed to seiche modes or the natural oscillations of Monterey Bay. Lynch attributed the 55-min oscillation to the fundamental longitudinal mode, the 36-min period oscillation to the fundamental transverse mode, and the 27-min oscillation to a shelf wave. Schwing et al. (1990) examined tidal records following the Loma Prieta Earthquake in 1989, and found high-amplitude oscillations with periods in the range of 8–60 min that lasted for several days. They also identified one oscillation, with a period of about 9 min which they attributed to a natural mode of Monterey Harbor.

In a study of the tidal and non-tidal oscillations in Elkhorn Slough, an estuary directly connected to Monterey Bay, Breaker et al. (2008) found several higher frequency oscillations with periods of 55.4, 36.3, 27.3, and 21.5 min, consistent with the natural oscillations of the bay that had been identified in previous studies (e.g., Lynch, 1970). These oscillations were not transient, but, rather, tended to be continuous in nature.

Based on the studies indicated above, the natural oscillations of Monterey Bay appear to be essentially a continuous function of time. In most cases, where seiche modes have been observed, they are transient in nature and last for only a short period after the forcing or excitation has terminated. Although weather-related events do contribute to the natural oscillations, another mechanism may be responsible for producing them on a continuous basis.

In this study, we use two different numerical models to aid in our understanding of seiching in Monterey Bay. One model employs idealized wind forcing and realistic bathymetry to explore the resonant characteristics of Monterey Bay while the other model includes tidal forcing and is used to simulate spatial patterns associated with the various natural modes, and the response due to realistic wind and tidal forcing. The main purpose of this study is to re-examine the natural oscillations of Monterey Bay based on new observations and to investigate how they are generated. Finally, this study not only presents a number of new results but also summarizes most, if not all, of the past work that has been done on the subject of the natural oscillations of Monterey Bay and so should serve as a useful reference in future studies.

2. Observations and analyses

2.1. The natural oscillations of Monterey Bay excited by earthquakes

2.1.1. The Loma Prieta Earthquake of 1989

On October 18, 1989 at 0104 GMT, a magnitude 7.1 earthquake occurred on the San Andreas fault in the Santa Cruz mountains approximately 16 km northeast of Santa Cruz, California (McNutt, 1990). This event generated a tsunami in Monterey Bay that was recorded at the tide gauge in Monterey Harbor, approximately 20 min after the main event (Schwing et al., 1990). Several mechanisms have been proposed that may have caused the event (Breaker et al., 2009). Ma et al. (1990) produced a synthetic tsunami for the bay based on the seismic characteristics of the earthquake, and concluded that faulting, submarine slumping within the bay, or local slumping near Moss Landing could have generated a tsunami similar to that observed at Monterey.

Fig. 2a shows the tide gauge record for the 3-day period from 18 to 21 October, 1989 (Breaker et al., 2009). In Fig. 2b, a 5-h segment of this record has been extracted for closer inspection. The primary response to this event appears to have taken place during the first 10–15 h after its arrival (Schwing et al., 1990). The maximum range of variability during the first 5 h approaches 45 cm. However, due to the response characteristics of the tide gauge employed and the subsequent data processing, this record may

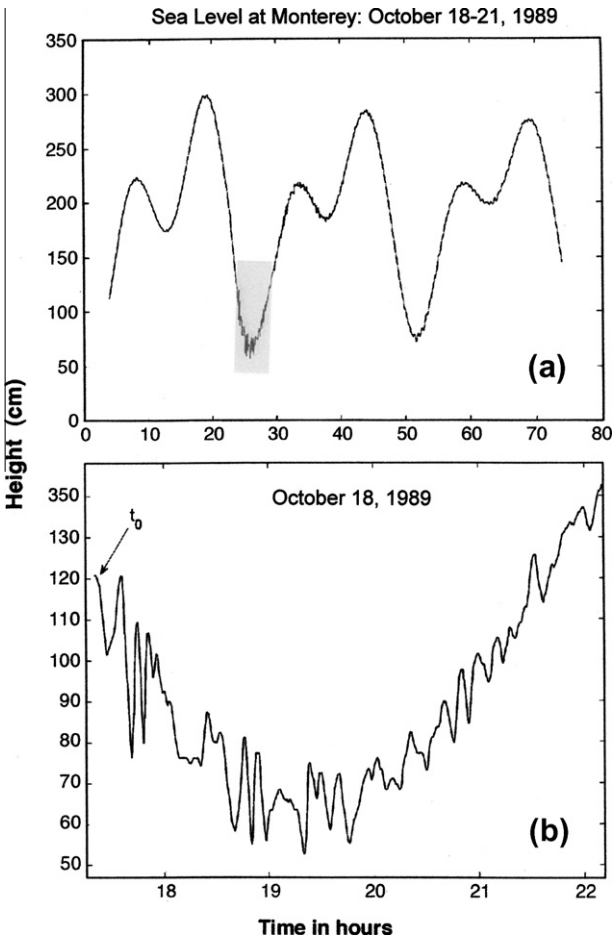

Fig. 2. (a) The sea level record from the tide gauge in Monterey Harbor for the Loma Prieta Earthquake for the period October 18–21, 1989. The first 5 h of this event are highlighted in gray (a) and are shown in detail below (b), where t_0 represents the initial arrival of the tsunami signal at the tide gauge.

underestimate the true amplitudes of the signal by as much as 50% according to Schwing et al. (1990).

Singular Spectrum Analysis (SSA) was applied to this record in order to extract the primary frequencies. A detailed account of the method is given in Golyandina et al. (2001). It is well-suited for decomposing relatively short, noisy records. Two frequencies were identified in the decomposition, the first with a period of 9–10 min, and the second with a period of 31–32 min. The period of 9–10 min was also indicated in the results of Schwing et al. (1990). A period of 31–32 min corresponds, at least approximately, to one possible mode of oscillation that has been predicted for Monterey Bay, and in the case of the 9–10 min oscillation, for Monterey Harbor, based on the results of WHK.

2.1.2. The Great Alaskan Earthquake of 1964

On March 28, 1964 at 03:36 (GMT), a shallow earthquake of magnitude 8.4 occurred at 61.0°N, 147.8°W in Prince William Sound, in south-central Alaska (Page, 1968). Uplifting caused vertical displacements as large as 16 m on the sea floor in the vicinity of the epicenter (Malloy, 1964). During the first day following the main event there were 11 aftershocks of magnitude 6.0, or greater, but none of the aftershocks were of sufficient magnitude to generate a second tsunami. The tsunami that was generated by this earthquake propagated south along the west coast of North America and reached the latitude of Monterey Bay at approximately 08:18 (GMT) on March 28, 1964.

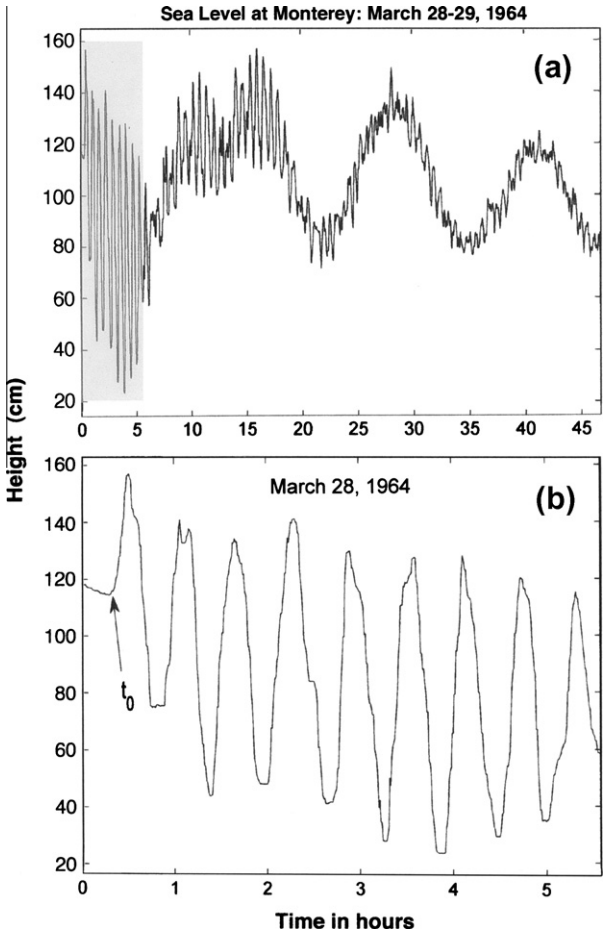

Fig. 3. (a) The sea level record from Monterey Harbor for the Great Alaskan Earthquake for a 47-h period from March 28 to 29, 1964. The first 5 h of this event are highlighted in gray (a), and are shown in detail below (b), where t_0 again represents the initial arrival of the signal associated with the tsunami at the tide gauge.

Fig. 3a is a digitized version of the strip chart that was originally recorded from the tide gauge in Monterey Harbor for the 2-day period following the first arrival of this event, i.e., t_0. Fig. 3b shows the initial 6-h portion of this record highlighted in gray in Fig. 3a. The range of the maximum oscillations associated with this event approaches, or even exceeds, 100 cm, and thus is similar in amplitude to that of the semidiurnal tide. However, we do not know how realistic these amplitudes are since there is no record of the tide gauge that was used or its response characteristics. Over the first 2 days the amplitudes of the oscillations decreased by roughly an order-of-magnitude. Oscillatory behavior associated with this event was detected for at least 4 days following the main event and have been attributed to various multi-path arrivals that are described in Breaker et al. (2009).

SSA was applied to this record as well. The SSA decomposition in this case yielded several modes, all with a period of approximately 37 min. An observed oscillation with a period of approximately 37 min agrees well with past observations, and more recent observations that are presented in the following section. This period corresponds to the expected transverse mode of oscillation for the bay that assumes a nodal line across the entrance from Pt. Piños to Pt. Santa Cruz. It is consistent with a long-period gravity wave that enters the bay from the west, and as it conforms to the bay's physical dimensions, is transformed through quarter-wave resonance into a seiche whose period has been approximately predicted by WHK.

2.2. Tide gauge and pressure data

The data used in this study come from two sources, water levels from the National Ocean Service[2] (NOS) tide gauge in Monterey Harbor (Station number 9413450), and pressure data from the Pier in Santa Cruz provided by the Network for Environmental Observation of the Coastal Ocean (NEOCO) program have also been drawn upon. The tide gauge data from Monterey Harbor cover the period from 6/12/2002 to 8/12/2003. These data were collected every 6 min, providing 240 observations per day. The pressure data from the Santa Cruz Pier were acquired from a CTD instrument located next to the pier at a depth of 5 m. These data were collected during a 17-month period during 2003 and 2004, although we have used only one portion of this record due to quality control issues. The data from the Santa Cruz Pier were collected every 4 min, providing 360 observations per day. The segment chosen for analysis spans the 77-day period from 1/28/2004 to 4/13/2004. Because the units associated with the pressure data from Santa Cruz were given in decibars and the sea level data from Monterey Harbor in millimeters, we have standardized the data from both locations (i.e., removing the means and dividing by the standard deviations), as is often done when the units differ (and even when they do not).

2.2.1. Data analysis

In order to identify the oscillations that are most likely related to the natural oscillations of Monterey Bay, we have initially calculated power spectra of the pressure data from the Santa Cruz Pier and water levels from Monterey Harbor (Fig. 4a and b). Power spectra were calculated using the Multi-Taper Method (MTM) of Thompson (1982, 1990) and the method of Welch (1967). The MTM is a modern non-parametric method of spectral analysis that is widely used. It is based on the periodogram. The method employs a series of windows called Slepian sequences that are used to taper the time series and thus reduce leakage. The number of tapers usually varies between 2 and 8. According to Weedon (2003), the effect of tapering is to produce a spectrum with well-sup-

[2] http://tidesandcurrents.noaa.gov/.

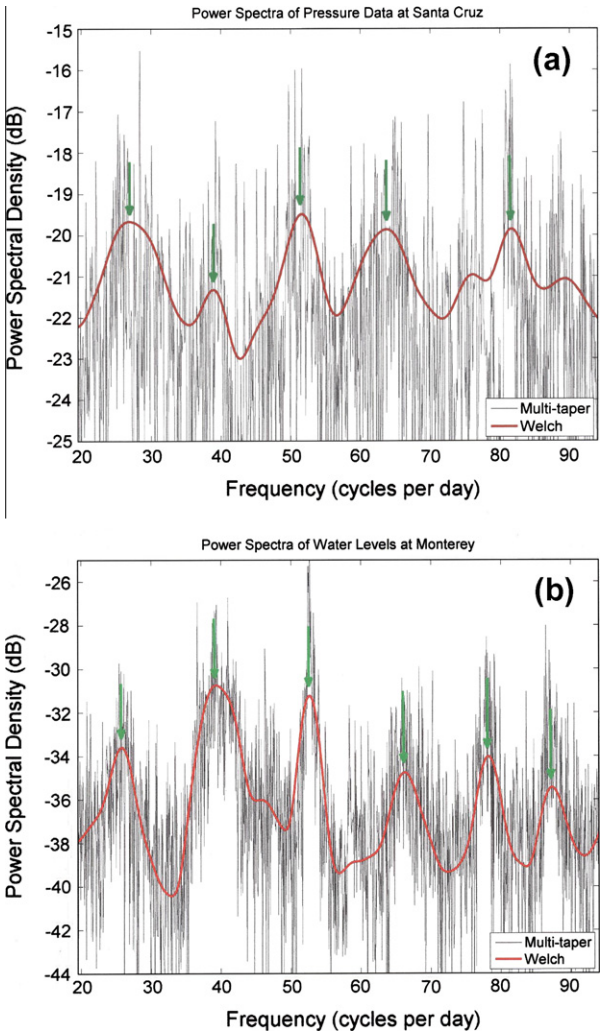

Fig. 4. (a) Power spectra of pressure data from the Santa Cruz Pier for the period from 1/28/2004 to 4/13/2004. The black trace shows the Welch power spectrum and the red trace shows the multi-taper power spectrum. Five primary spectral peaks at 26.8, 38.9, 51.6 63.7 and 81.7 cpd are identified by vertical green arrows. (b) Power spectra of sea level from Monterey Harbor for the period from 6/12/2002 to 8/12/2003. The six primary spectral peaks at 25.8, 39.3, 52.6, 66.2, 78.2, and 87.3 cpd are, again, shown by vertical green arrows. In both figures, the vertical axes are expressed on a logarithmic scale in deciBels (dB). (For interpretation of the references to colour in this figure legend, the reader is referred to the web version of this article.)

pressed side lobes and good smoothing, without sacrificing resolution. The number of tapers was set equal to 3, and the length of the Fast Fourier Transform (FFT) used to calculate the spectral estimates was set to 2^{12}, in each case. The Welch power spectrum is based on a modified periodogram where the data are divided into overlapping segments. A Hanning window is applied to compute the modified periodogram for each segment. The purpose of the window is to reduce the effect of side lobes and to decrease the estimation bias, which results in a slight decrease in resolution. In our case, a Hanning window with a length of 150 was employed. The purpose of the overlapping segments is to increase the number of segments that are averaged for a given record length, and thus to decrease the variance associated with the estimated Power Spectral Density (PSD). In our case, an overlap of 65 (i.e., 50%) was chosen. A length of 2^{12} was again chosen for the FFT. This also made it possible to directly overlay the MTM and the Welch PSDs. The Welch procedure is well-suited for estimating power spectra where the signals are relatively weak and not well-defined, which is true in our case. It is especially helpful in estimating the frequencies of interest rather precisely, and the signal-to-noise ratios (SNRs), as well. We refer to SNRs estimated from the Welch PSDs as "apparent", since they will depend, to some degree, on the parameters that are chosen to implement the method. We express the PSDs in deciBels (dB) since this facilitates comparing SNRs that are usually expressed in dB.

In Fig. 4a, the MTM (black) and Welch (red) spectra at Santa Cruz are shown, for the period from 1/28/2004 to 4/13/2004, or 2.5 months. Based on the Welch spectrum, five spectral peaks (indicated by vertical green arrows) at approximately 26.8, 38.9, 51.6, 63.7, and 81.7 cycles per day (cpd) have been identified. These frequencies have corresponding periods of 53.7, 37.1, 27.9, 22.6, and 17.6 min. For most of this study we focus our attention primarily on the four lowest frequencies. The signals of interest are not well-defined and are poorly resolved, consistent with SNRs that are relatively low. Thus, the advantages of the Welch power spectrum compared to the MTM in this case become readily apparent. The SNRs vary from roughly 1 to 3 dB and so must considered relatively small.[3] More precise estimates of the frequencies and periods, and the SNRs are given in Table 1. Fig. 4b shows the MTM and Welch PSDs for the water levels from Monterey Harbor, based on the period from 6/12/2002 to 8/12/2003, or a period of 14 months. In this case, six spectral maxima have been identified (again, by vertical green arrows). The frequencies associated with these maxima are approximately 25.8, 39.3, 52.6, 66.2, 78.2, and 87.3 cpd, with corresponding periods of 55.9, 36.7, 27.4, 21.8, 18.4, and 16.5 min. More precise estimates are given in Table 1. Although none of the spectral peaks at either location are statistically significant at the 5% level of significance, according to Tukey (1961), there is no substitute for repeated occurrences as a basis for establishing the existence and significance of spectral maxima. At Monterey, the SNRs range from 3.4 to 8.1 dB, and thus are significantly higher than the SNRs at Santa Cruz. When we compare the first five periods from Santa Cruz and Monterey (53.7 vs. 55.9, 37.1 vs. 36.7, 27.9 vs. 27.4, 22.6 vs. 21.8, and 17.6 vs. 18.4) we see that they are similar. Given the fact that these signals are small in amplitude and not well resolved in frequency, they most likely represent the same oscillations. Finally, the SNRs at Monterey are significantly higher in all cases than they are at Santa Cruz. Although the signal strength appears to be higher at Monterey than it is at Santa Cruz, it is not clear if the signal strength at Santa Cruz is actually lower, or whether the noise level is simply higher.

Most of these periods are similar, but not identical to, the spectral maxima identified by Lynch (1970) and Breaker et al. (2008). Breaker et al. (2008) identified four oscillations in Elkhorn Slough that were attributed to the natural oscillations of Monterey Bay. They occurred at 26.0 cpd (55.4 min), 39.7 cpd (36.3 min), 52.7 cpd (27.3 min), and 66.9 cpd (21.5 min). The 55-min period most likely corresponds to the first longitudinal mode and the 36-min period to the first transverse mode. The 27-min oscillation corresponded to a shelf wave, according to Lynch (1970), but could also correspond to the lowest mode of oscillation for the case where the bay was assumed to be triangular with a uniformly sloping bottom, according to WHK. Breaker et al. (2008) also noted that an oscillation with this period is an approximate multiple of the oscillation at 55 min and so could be a harmonic rather than a fundamental mode. An oscillation in the neighborhood of 22 min appears frequently in the model results of WHK and could, for example, correspond to an unsymmetric bimodal oscillation in the longitudinal direction.

[3] Actually, all we can estimate is the signal plus noise-to-noise ratio, or $(S+N)/N$, since we do not have a reliable estimate of the noise background at any specific frequency. However, for comparison with the data from Monterey we still find this approximation for the SNR useful.

Table 1
Properties of the spectral maxima at Santa Cruz and Monterey.

	Santa Cruz					Monterey					
Frequency (cycles per day)	26.81	38.85	51.59	63.72	81.65	25.78	39.26	52.62	66.21	78.16	87.30
Period (minutes)	53.71	37.07	27.91	22.60	17.64	55.86	36.68	27.37	21.75	18.42	16.49
SNR* (dB)	2.4	1.2	2.9	2.2	1.3	6.6	8.1	7.3	4.7	5.2	3.4

* Noise levels were estimated by taking the average of the levels on each side of the spectral peaks.

Generally consistent with previous observations, oscillations with the periods given above are observed at Monterey and Santa Cruz, reflecting their bay-wide nature. Although oscillations in these spectra occur at higher frequencies, they may in some cases be harmonically related to the lower frequency oscillations, and they occur at frequencies that are too high to be resolved by the models that we subsequently employ. Also, the higher modes of oscillation tend to be confined to separate parts of the bay and not to the bay as a whole, as we will see in the following section. That oscillations with similar periods occur at both ends of the bay, suggests that the canyon does not necessarily act as a barrier at these frequencies, although it might serve as a more effective barrier at higher frequencies.

To examine the continuous nature of these oscillations, a moving Fourier transform window has been applied to the same 14-month period of water levels from Monterey Harbor used in the previous figure to produce a spectrogram that, in addition to amplitude and frequency, is also a function of time (Fig. 5). It was calculated using a window length of 2^{11}, and the percent of overlap between successive windows was 50%. The number of points used in calculating the FFT to obtain the PSDs was 2^{11}. The range of frequencies displayed extends from 10 to 76 cpd, and so excludes the primary tidal constituents. Higher amplitudes occur at approximately 26.0, 39.7, 52.7, and 66.9 cpd. These frequencies generally agree with those observed by Lynch (1970), who attributed them to the natural frequencies of Monterey Bay and their harmonics, those observed by Breaker et al. (2008), and at least some of the frequencies predicted by WHK. Major weather-related events that affect the entire spectrum occur in early-to-mid November 2002, mid-to-late December 2002, January 2003, and mid-to-late March 2003. Synoptic maps of surface pressure verified that the events in November, December, and March were all associated with winter storms with higher winds and lower barometric pressures (Warren Blier, personal communication). A detailed comparison of maxima in the surface winds from NDBC Environmental Data Buoy 46042, located just outside Monterey Bay, showed close agreement with the events in sea level (within ±1–2 days) during the major storm periods in December and March but less agreement at other times. These events represent the type of transient forcing that we usually expect to excite seiche oscillations in lakes and bays. Of particular note, however, is the continuous nature of the oscillations at the four lowest natural frequencies. Although these signals are essentially continuous, they are relatively weak, with amplitudes on the order of millimeters.

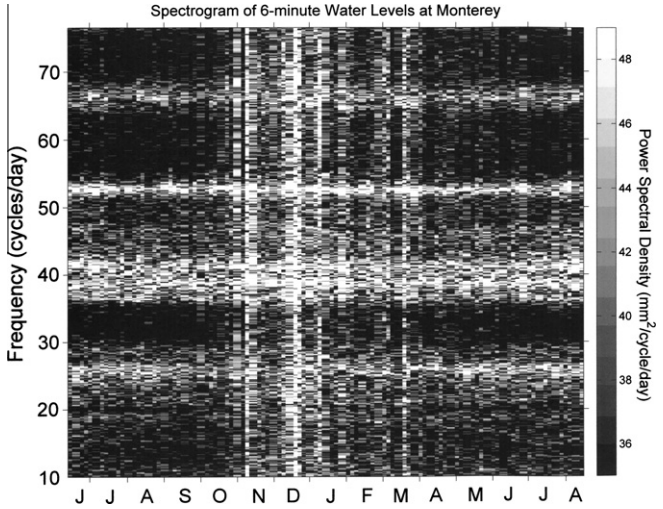

Fig. 5. The moving spectral window or spectrogram for the sea level data from Monterey Harbor. The frequency ranges from 10 to 76 cpd. It is important to note that the tick marks along the *x*-axis are located at the *center* of each month. A gray scale that displays the Power Spectral Density in mm^2/cycle/day is shown at the right. See text for details.

To examine these oscillations in greater detail we have filtered the data from Monterey Harbor using band-pass filters centered at 25.8, 39.3, 52.6, and 66.2 cpd. Specifically, we have applied a Butterworth Infinite Impulse Response (IIR) band-pass filter to the data (Parks and Burrus, 1987). Four parameters determine the filter's performance, width of the pass band or bandwidth, its smoothness (i.e., ripple), width of the stop bands, and the stop band attenuation. These parameters have been chosen to produce a filter response that is smooth with a relatively narrow pass band, centered at each of the four lowest frequencies. The bandwidth was set at 0.02 cpd at each frequency. A constant bandwidth was chosen so that the signal response at each frequency could be directly compared since the response time of the filter is inversely proportional to the bandwidth. The results are shown in Fig. 6 where the amplitudes are expressed in millimeters. Several peaks occur between November 2002 (~2002.8) and March 2003 (~2003. 2). In each case they correspond to the winter storm events referred to earlier. There is a slight tendency for the response to the storm events to increase proceeding from 25.8 cpd (top panel) to 66.2 cpd (bottom panel). The greatest response corresponds to the event in mid-December where the amplitude at 66.2 cpd is at least twice the amplitude at 25.8 cpd.

2.3. Observed damping in Monterey Bay

The effects of damping on the natural oscillations of Monterey Bay can be estimated from the previous power spectra by calculating the quality factor, *Q*, defined as

$$Q = f_0/\Delta f. \quad (4)$$

where f_0 is the center frequency and Δf, the bandwidth (e.g., Crowell, 2006). Δf is defined as the width in frequency where the energy has fallen to one half of its maximum value. *Q* represents the number of oscillations required for the energy to decay to approximately 0.2% of its original value when impulsive forcing is applied. A complete explanation of *Q* and its relation to damping is given in Jackson (1962). Strong damping occurs when an oscillation loses half or more of its amplitude with each succeeding cycle. To calculate *Q*, we obtained values for f_0 and Δf from the Welch power spectra shown in Fig. 4. The values of *Q* for the four frequencies of primary interest increase from roughly 4 to 8 for center frequencies of 26.0, 39.7, 52.7, and 66.9 cpd, respectively. Although *Q* increases because f_0 increases, the bandwidth remains essentially constant. These values do not indicate a high degree of resonance, but rather, a system with at least moderate-to-strong damping. It is interesting

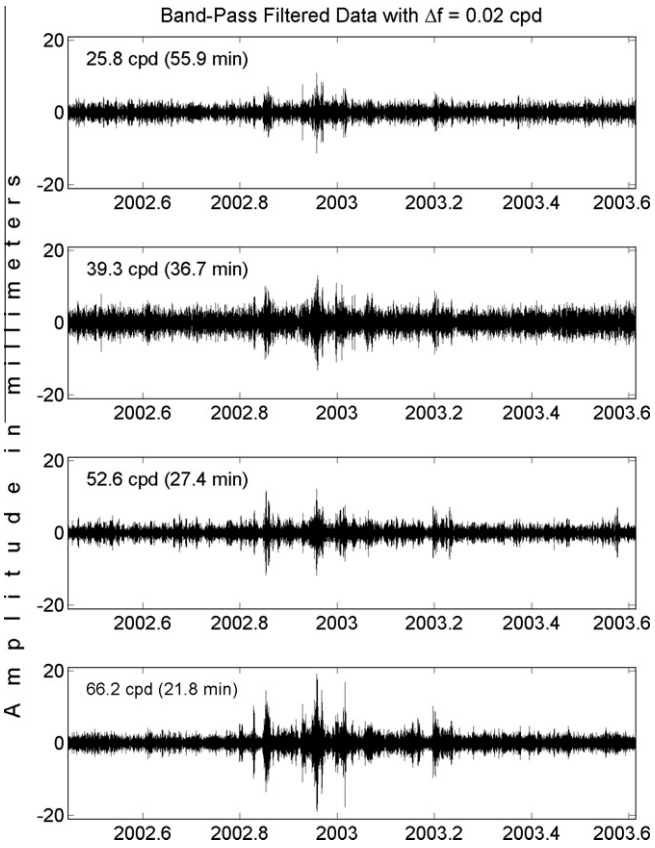

Fig. 6. The band-pass filtered data are shown for the four lowest frequencies of interest. The bandwidth is 0.02 cpd in each case. The four panels from top to bottom show the filtered data at 25.8 cpd (55.9 min), 39.3 cpd (36.7 min), 52.6 cpd (27.4 min), and 66.2 cpd (21.8 min), respectively. Amplitudes are expressed in millimeters (mm). See text for details.

to compare these values with Neumann and Pierson (1966) who state that in most cases, seiches do not last for more than 5 or 6 cycles, implying the degree to which the ocean itself imposes the damping.

3. Numerical results based on idealized and realistic forcing

In order to obtain a better understanding of the natural oscillations of Monterey Bay, we employ two numerical models to investigate the processes that may be responsible for producing the observed modes of oscillation. We employ two models because each has certain advantages. The first model, the Monterey Bay Area Regional Model (MBARM), is used to impose impulsive wind forcing. It employs high resolution bathymetry with no smoothing. This may be significant since the periods associated with the natural oscillations will, to some extent, be affected by any bathymetric smoothing that is applied. This model is described in greater detail in the following section. The second model, the Regional Ocean Modeling System (ROMS) falls into this category. The steep topographic gradients encountered in Monterey Submarine Canyon highlight this problem. The ROMS is used to impose realistic forcing which includes the winds and tides. It is unique in that it is the only regional model that includes tidal forcing in Monterey Bay, and tidal forcing is one of the forcing mechanisms we investigate. This model is described in greater detail in Section 3.3.

3.1. Sensitivity of the bay's response to impulsive wind forcing

First we describe the MBARM model we employ to impose impulsive wind forcing. The version of the model used is non-hydrostatic although for the purposes of this study no significant differences with the hydrostatic version should be expected. The model uses a blend of collocated and staggered grid structures (mixed Arakawa A and C grids). With a time step of 1.7 min and the constraints imposed by the numerical approximations employed, the highest frequency that can be fully resolved by the model has a period of approximately 20 min. This is a conservative estimate based on the premise that at least eight samples per cycle are required to completely resolve oscillations with periods of this order. Fourth-order central differencing is used in the control volume approximation to compute all advection and horizontal pressure gradient terms, except adjacent to boundaries where second-order accuracy is used. Vertical viscosity and diffusivity are the sum of the terms which parameterize laminar diffusivity and the vertical Reynolds stresses as given by Pacanowski and Philander (1981). The horizontal eddy viscosity and diffusivity are 20 m^2/s. This gives a damping time of nearly a month for disturbances on the scale of 10 km. A detailed description of the model and the non-hydrostatic solver can be found in Tseng (2003) and Dietrich and Lin (2002).

The model employs a z-level vertical coordinate system and is one-way coupled to the larger scale California Current System (CCS) model (Haney et al., 2001) and uses the immersed boundary method based on boundary fluxes to represent the coastal geometry and bathymetry (Tseng and Ferziger, 2003, 2004). Thus, realistic bathymetry with no smoothing can be employed which is particularly important in the region of the Monterey Submarine Canyon. The bathymetric data used in the model is from Wong and Eittreim (2001), and is unfiltered, with a resolution of 250 m. A pure upwind advective scheme is used at the three lateral open boundaries (north, south, and west) for all variables. The open boundaries allow perturbations generated inside the MBARM domain to exit without deterioration of the model solution and also allows information from the CCS model to advect inward. External forcing from the CCS model is advected inward as an inflow boundary condition, and the interior model results are advected outward as an outflow boundary condition. The model is initialized after the MBARM reaches quasi-steady state conditions. For more details, see Tseng and Breaker (2007), Tseng et al. (2005), and Haney et al. (2001).

Sudden changes in wind forcing are expected to cause seiching in many semi-enclosed embayments including Monterey Bay. The winds in Monterey Bay are predominantly from the northwest between March and October, but are more variable in speed and direction during the winter months (e.g., Breaker and Broenkow, 1994). In the model simulations that follow, we vary the impulsive wind forcing according to wind direction by octant, from the north, northwest, west, southwest, and finally, from the south (Fig. 1). The wind forcing is also varied according to impulse duration and location within the bay. The oscillations that result from impulsive wind forcing from the MBARM-simulated equivalent sea surface heights, i.e., surface elevations relative to still water, are based on sea surface pressure via the hydrostatic approximation.

First, impulsive wind forcing is imposed for several forcing periods. The wind has been converted to wind stress and a constant value of 5 dynes/cm^2 has been applied in each case. The wind forcing is turned on at one time step and then turned off 15, 30, and 60 min later.

Different forcing periods were employed because the impulses take the form of a square wave and, based on the principles of Fourier analysis, the frequencies that make up the square wave will depend on the forcing period that is chosen. Forcing periods of less than 15 min were also employed, but the results were of less interest because the responses were far smaller than those obtained for periods of forcing that were 15 min or longer. The direction of wind forcing is from the west in each case, a choice based on results pre-

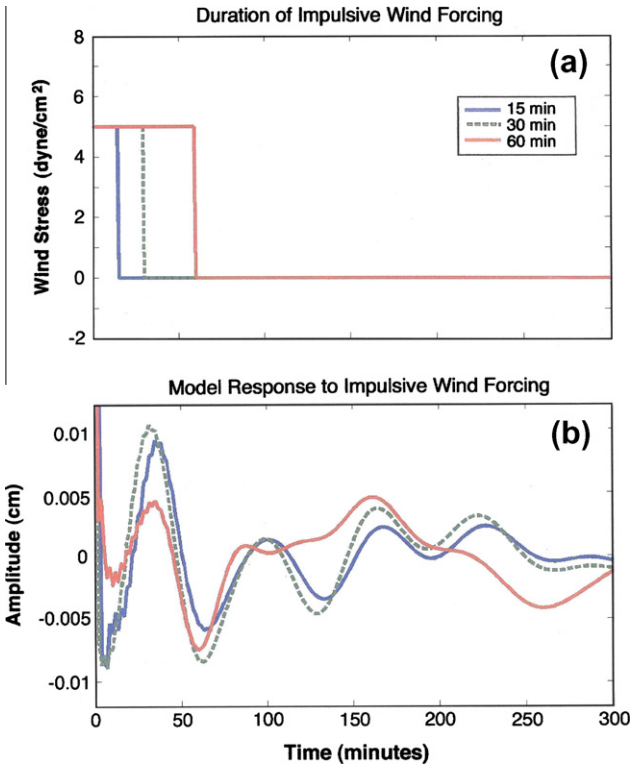

Fig. 7. The upper panel (a) shows the periods of impulsive wind forcing used in the MBARM model, 15 (blue), 30 (green-dashed), and 60 (red) minutes. The lower panel (b) shows the model response in equivalent sea surface height (cm) in the southern half of Monterey Bay (Fig. 1 – the black diamond). (For interpretation of the references to colour in this figure legend, the reader is referred to the web version of this article.)

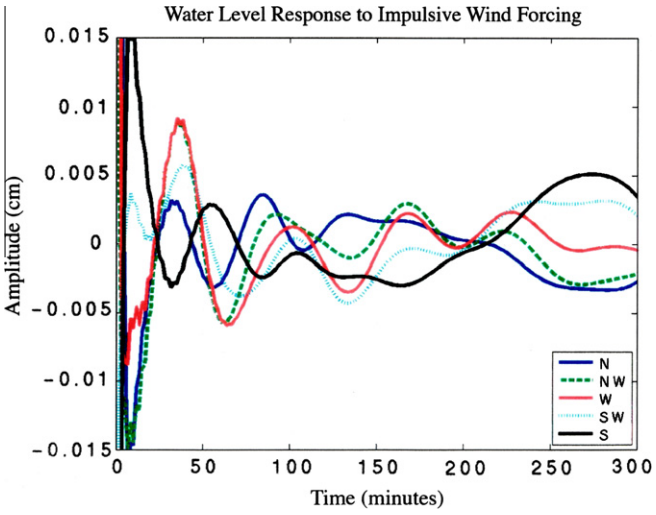

Fig. 8. The transient oscillations generated by the MBARM model for impulsive wind forcing from the five directions shown in Fig. 1. The range in amplitude has been truncated at ±0.015 cm.

sented in the next paragraph. The periods of impulsive wind forcing are shown in Fig. 7a, and the model responses to the wind forcing in Fig. 7b. The response is measured in terms of model-generated surface elevations for a grid point located in the southern half of Monterey Bay and slightly toward Monterey at 36.7°N, 121.96°W (Fig. 1, black diamond). Although higher amplitudes occur at other locations, our primary interest is in the relative response to changes in the forcing period. Thus, we assume that similar relative responses would occur at other locations and that the optimum forcing period is independent of location. At periods of 15 and 30 min, the model-generated oscillations have a period of approximately 50 min, whereas for the 60-min forcing, the oscillation period is somewhat shorter. Overall, the strongest response occurs at a forcing period of 15 min, and as a result we use this forcing period in all subsequent model simulations.

Second, we impose the wind from five different directions: north, northwest, west, southwest, and south (Fig. 1). The same wind stress of 5 dynes/cm^2 was employed in each case. The wind was turned on at one model time step and turned off at a time step 15 min later. The results are shown in Fig. 8. Of primary interest are the amplitudes, the number of oscillations produced, and the periods associated with them. These values are presented in Table 2. Since the actual time between adjacent cycles was not always constant we have taken the mean time between cycles to estimate the period. The results indicate that the highest amplitude oscillations occur for winds from the west and northwest. The number of cycles generated range from 2 to 3 for winds from the south, to almost five cycles for winds from the west, before they completely decay, consistent with the results of the quality factor analysis in Section 3.3. Based on the amplitudes and numbers of oscillations produced, the strongest responses to impulsive wind forcing appear to be for winds from the west and northwest. The periods range from 50 to 79 min. The longest periods occur for winds from the west and southwest. From Table 2 we also note the symmetrical nature of the results for wind forcing from the north and south. The amplitudes, number of oscillations and periods are similar. The periods, in particular, are generally consistent with the first longitudinal mode predicted by WHK with a period of 44.2 min, and the lowest observed frequency with a period of 55 min. Thus, wind forcing (or changes in wind forcing) from the north or south that are approximately aligned with the longitudinal axis of the bay may be most effective in generating the first mode of oscillation.

We stated initially that the natural oscillations of any basin are not influenced by the nature of the forcing. The results presented above might appear to contradict this fact. However, several factors almost certainly influence the periods that have been predicted. First, wave interactions between different modes and reflected oscillations may come into play. Second, different modes are excited at different locations within the bay because of its geometry. Also, the *effective* dimensions of the bay that are relevant in a given situation may differ slightly from the true dimensions, depending on the nature of the forcing. This is especially true in this case due to the presence of a relatively large submarine canyon that bisects the bay and the complex bathymetry associated with it.

Next, we examine the response to impulsive wind forcing from the west of 15 min duration for the three locations along longitude 121.96°W (Fig. 1): just north of Pt. Piños at the south end of the bay (36.7°N; black diamond), over the MSC near the center of the Bay (36.8°N; black circle), and just south of Santa Cruz, at the north end of the bay (36.92°N; black square). Previous work (WHK) and our own observations have suggested that the natural oscillations of Monterey Bay can differ significantly for different locations. For example, the canyon itself may separate the bay into separate oscillating basins producing resonant behavior that differs at each end of the bay, although the results shown in Fig. 4 do not necessarily support this argument. To explore the influence of MSC on the oscillating characters of the bay, we have removed the canyon, limiting the maximum depth to 300 m (Fig. 9). At the south end of the bay, the response is about the same, with, or without, the canyon, although there is a slight phase difference initially. The amplitudes decay significantly after four oscillations. The period in this case is about 40 min. At the center of the bay, the

Table 2
Properties of the model-simulated oscillations for five different wind directions.

Wind direction	Maximum amplitude* (cm)	Number of oscillations	Mean period (min)
North	0.032	3–4	50
Northwest	0.08	4	55–60
West	0.085	4–5	67
Southwest	0.06	3	79
South	0.03	2–3	50

* The maximum amplitudes were estimated from the first complete cycle following the impulse.

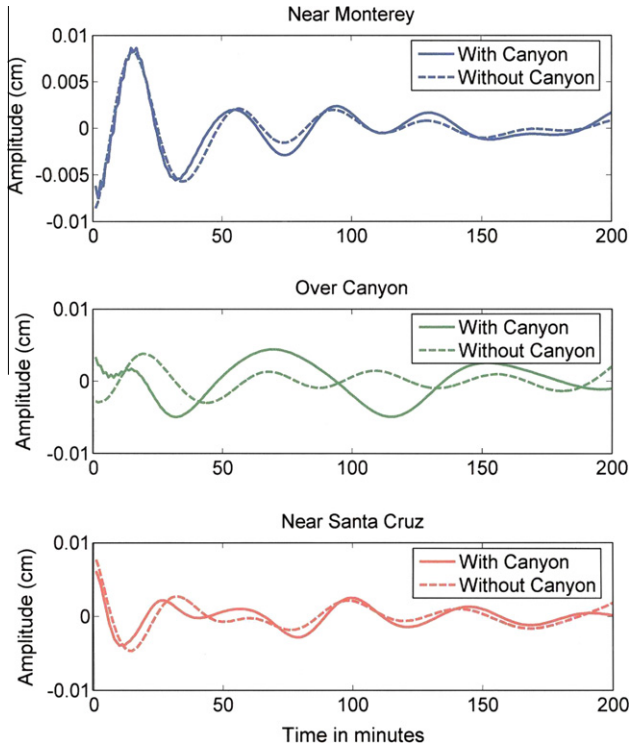

Fig. 9. The MBARM model response (centimeter) to impulsive wind forcing for the three different locations in Monterey Bay shown in Fig. 1: (a) the southern half of the bay "Near Monterey" (36.7°N, 121.96°W), (b) the center of the Bay "Over Canyon" (36.8°N, 121.96°W), and (c), the northern half of the bay "Near Santa Cruz" (36.92°N, 121.96°W). The wind forcing was applied for a period 15 min and the direction was from the west, in each case. The solid lines show the response with the Canyon, and the dashed lines show the response without the Canyon.

situation is quite different. There are significant differences in amplitude and phase, with, and without, the canyon. The amplitude is several times larger with the canyon and the period is about 83 min, compared to roughly 48 min, without the canyon. When the impulsive wind forcing is applied at the center of the bay, the canyon clearly has a major effect on both the amplitude and period of the oscillations. At the north end of the bay, the response is about the same, with, or without, the canyon, and again there is a slight phase difference, initially. Also, the amplitudes are slightly smaller, consistent with our observations at each end of the bay (Fig. 4). In this case, the mean period is approximately 45 min.

3.2. Comparing the predicted modes of oscillation with model simulations that employ idealized wind forcing

Here, we blend and compare the model results obtained from the idealized wind forcing with the predicted modes of oscillation from WHK. The classical analyses of WHK which employed the methods of Stoker (1957) are presented in Appendix A. As indicated, the first mode has a predicted period of 44.2 min, and the oscillating pattern is confined to the northern half of the bay, apparently isolated from the southern half of the bay by the presence of the MSC. A period of 44.2 min is very close to the ~45-min period predicted by the MBARM when impulsive wind forcing was applied at the north end of the bay near Santa Cruz.

In Fig. 10, maps of simulated equivalent sea surface height or surface elevation relative to still water based on wind forcing from five directions, north, northwest, west, southwest, and south, are shown. The period of impulsive wind forcing is 15 min in each case. Several rather consistent patterns emerge. First, we see a boundary that resembles a nodal line that extends from Moss Landing out to the center of the bay and slightly beyond. This line is particularly well developed for winds from the north, northwest, and south, and almost certainly reflects the influence of MSC. This nodal line represents a boundary that separates seiche activity in the northern half of the bay, from seiche activity in the southern half, consistent with the first three modes shown in Fig. A2 from WHK where the oscillations are confined either to the northern half of the bay or the southern half.

Second, there are weaker indications of a nodal line that extends across the bay but located slightly further offshore than the nodal line shown in Fig. A1. This offshore nodal line is most apparent for wind forcing from the west. In this case, the nodal line could be located as much as 10 km further offshore. Such a large change in the position of the nodal line is probably unrealistic, plus it is not as clear where such a nodal line would be anchored at its extremities. However, this result differs from the assumed location employed by WHK, and might explain some of the discrepancies they found between their model results and observations. In several of the numerical analyses they conducted, for example, the first transverse period of oscillation ranged from 29.6 to 32.7 min, somewhat less than the periods of 36.8 and 37.1 min we observed at Santa Cruz and Monterey (assuming that we have identified the same mode), and the ~37-min period obtained from a frequency analysis of the tidal record at Monterey from the Great Alaskan Earthquake of 1964. By increasing the transverse distance between Moss Landing and the nodal line by only 5 km, the predicted modal period increases to a value of 35.8 min, using the same values used by WHK, in Eq. (3). However, there is another likely explanation for these discrepancies. For bays with wide openings to the ocean, it is often necessary to introduce a correction when the opening is an appreciable fraction of the length of the bay, in this case the distance between the nodal line and Moss Landing. According to Defant (1961), this correction becomes greater as the opening becomes larger in relation to its length. The corrected period becomes $T(1 + \varepsilon)$, when T is computed according to Eq. (1). ε is a function of several parameters which are given in Defant (1961) but will not be repeated here. Because there are several restrictions on just how this correction should be applied, it becomes difficult in practice to make this correction with a high degree of confidence.[4] In concept, however, if this correction could be determined and applied with confidence then this approach might be better than extending the nodal line further offshore in order to obtain better agreement between the observations and theory.

Finally, surface elevations appear to have antinodes in the northern and southern portions of the bay although they are out of phase. For winds from the N, NW, and W, surface elevations are negative at the northern extremity of the bay and positive, north of the Monterey Peninsula. For winds from the south, how-

[4] This may also explain why WHK did not attempt to use this approach in their analysis.

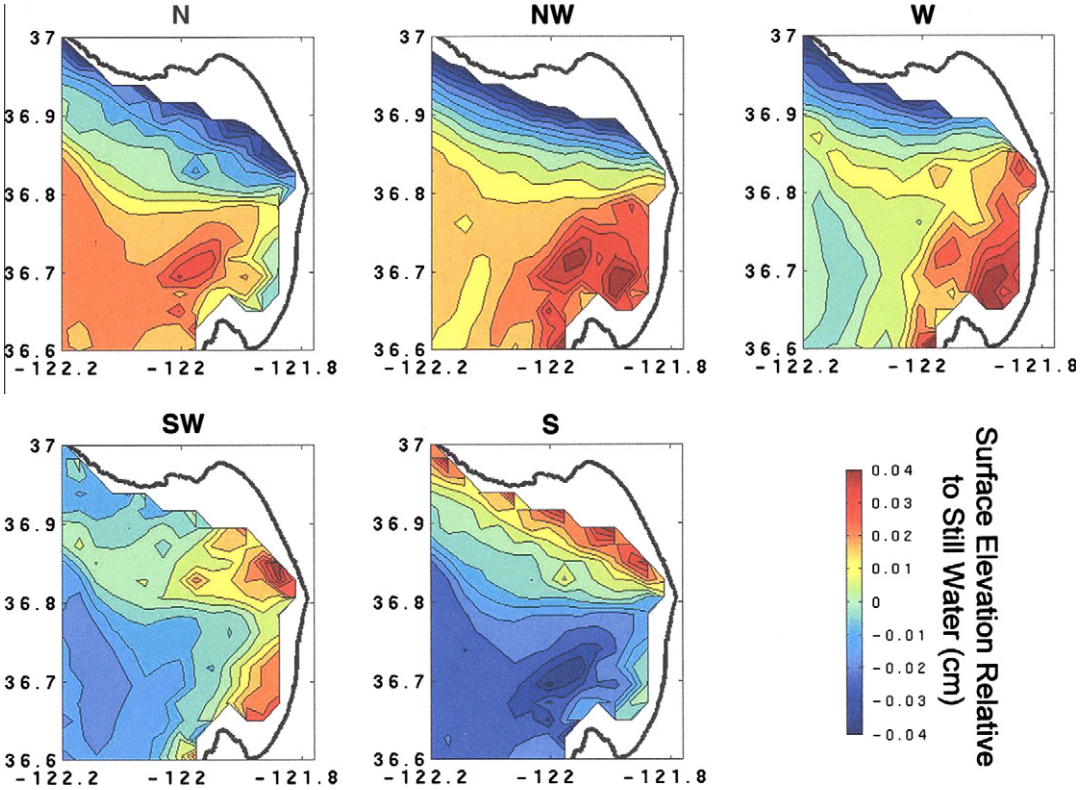

Fig. 10. The spatial patterns of surface elevation relative to still water (centimeter), i.e., equivalent sea surface height, generated by the MBARM model for impulsive wind forcing from the five directions, N, NW, W, SW, and S, shown in Fig. 1. See text for details.

ever, the opposite occurs, with positive elevations trending NW from Moss Landing in the northern half of the bay, and strongly negative elevations just north of the Monterey Peninsula. Seiching in the southern half of the bay near Monterey is clearly depicted in Fig. A2c for the third mode from WHK, where the predicted period was 28.2 min. More generally, local seiching is expected to occur in the vicinity of Monterey Harbor based on many of the model results obtained by WHK.

3.3. Simulated natural oscillations of Monterey Bay based on realistic forcing

We continue our study of the natural oscillations of Monterey Bay using ROMS which employs realistic forcing. The ROMS is a community model widely used for regional applications (Schepetkin and McWilliams, 2005). The model uses a generalized vertical coordinate system that follows the bottom topography (Song and Haidvogel, 1994). A curvilinear coordinate following the coast line is used in the horizontal plane. The model explicitly represents the time evolution of the free surface and has open boundary conditions to allow the exchange of information across them (Marchesiello et al., 2001). Vertical mixing is parameterized using the K-profile parameterization scheme, which accommodates potentially important physics related to ocean mixing (Large et al., 1994). The numerical grid for ROMS as it is implemented in Monterey Bay has a horizontal resolution of 600 m, with 40 levels along the vertical coordinate. The model time step is 1.5 min. The horizontal mixing coefficient is set to zero, where an up-stream advection scheme is used to account for horizontal mixing (Schepetkin and McWilliams, 2005). The atmospheric forcing is imposed hourly and includes the surface wind stress, and short wave and long wave radiation. The latent and sensible heat fluxes are computed from atmospheric temperature, relative humidity, and the ROMS sea surface temperature using the bulk formula of Kondo (1975). The atmospheric fields are provided by the Coupled Ocean/Atmosphere Mesoscale Prediction System (COAMPS; Hodur, 1997). Besides the atmospheric forcing, the model also includes tidal forcing with eight tidal constituents (M2, S2, N2, K2, K1, O1, Q1, P1) using the Flather boundary condition (Flather, 1976) along the southern, northern, and western boundaries. The tidal forcing is obtained from a global inverse barotropic tidal model (TPX06.0; Egbert and Erofeeva, 2002; Egbert et al., 1994), which uses an inverse modeling technique to assimilate satellite altimetry cross-over observations. ROMS is nested in the regional ocean forecast system (http://ourocean.jpl.nasa.gov/MB) which has three levels in the vertical and a horizontal resolution of 1.6 km (Wang et al., 2009). ROMS starts from a data-assimilated initial condition on August 1, 2006 using the model output from a previous forecast from the regional ocean forecast system for both the initial and boundary conditions after interpolation to the ROMS grid.[5] The atmospheric forcing is also provided for August 2006 when the wind direction is typically from the northwest and the speeds are of the order of 10 m/s.

We now examine the natural oscillations of Monterey Bay by calculating Power Spectral Densities (PSDs) at every grid point within the bay from ROMS 6-min sea surface heights and mapping the integrated PSDs for four frequency bands centered at 26.0 cpd, 39.7 cpd, 52.7 cpd, and 66.9 cpd (Fig 11). There were distinctive peaks in the PSDs at these frequencies in the model-generated sea surface heights (not shown), but higher frequencies were not well resolved. The bandwidth, as defined in Section 3.3, is 4 cpd

[5] Because the natural frequencies are not time-dependent, any period could have been chosen, and appropriate data were available for this period.

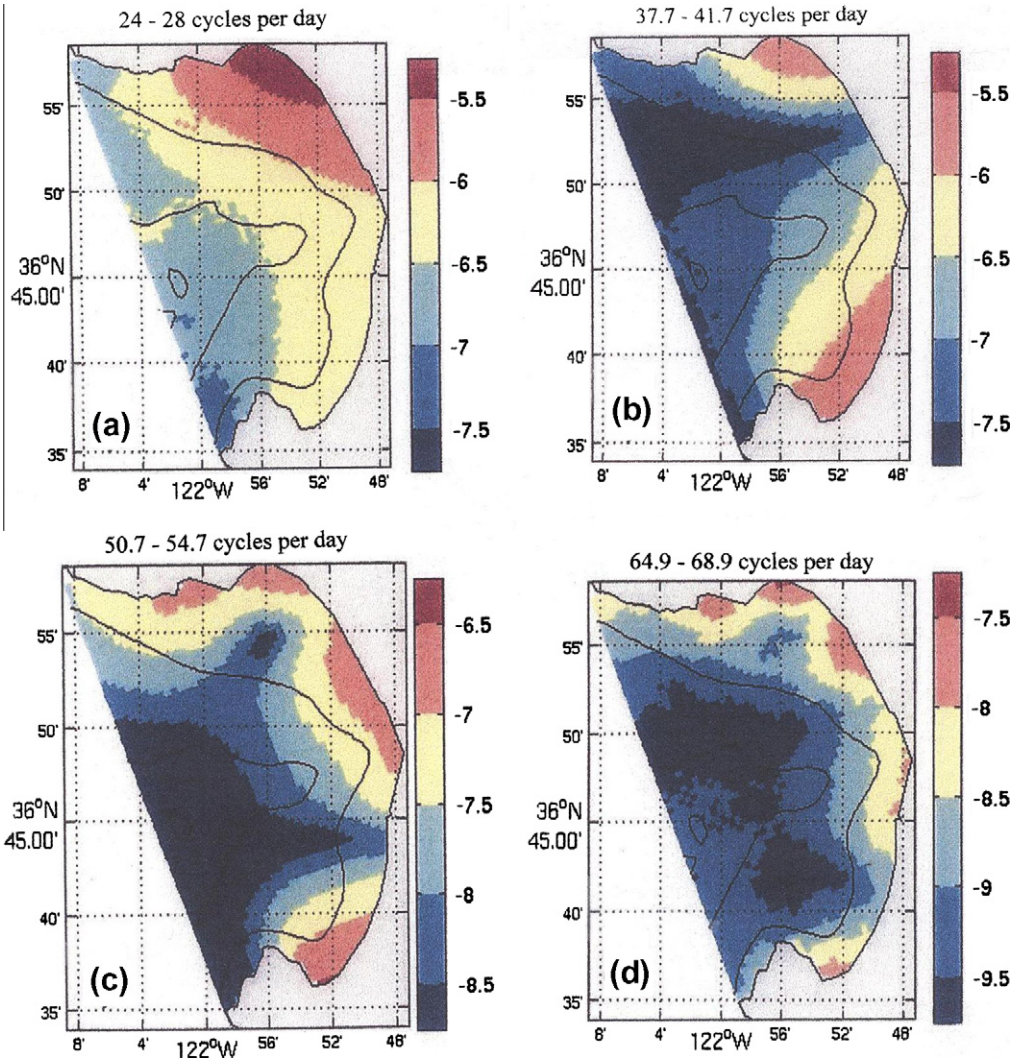

Fig. 11. Integrated power spectra of sea surface height from ROMS for Monterey Bay in four frequency bands: (a) 24–28 cpd, (b) 37.7–41.7 cpd, (c) 50.7–54.7 cpd, and (d), 64.9–68.9 cpd. The color bars show the variance in these frequency bands on a logarithmic scale. See text for details. (For interpretation of the references to colour in this figure legend, the reader is referred to the web version of this article.)

in each case. The PSDs were calculated using the method of Welch (1967), as described earlier. The model was integrated for 20 days and the last 5 days of model output are included in the spectrum analysis. The spatial distribution of integrated power spectra centered at 26.0 cpd (55.4 min) has a maximum at the northern end of the bay just east of Santa Cruz, and most likely reflects an antinode at this location. This pattern closely resembles the spatial pattern shown in Fig. A1, in Appendix A, which corresponds to the first 3D mode of oscillation based on the results of WHK. Although the patterns are similar, the period predicted for this mode by WHK is only 44.2 min. Because the pattern is primarily confined to the northern half of the bay, we may again infer that MSC plays a role. The spatial distribution of the integrated PSD centered at 39.7 cpd (36.3 min) reveals relatively large values near Santa Cruz, as before, and in the southern bay, near Monterey, as well, with a nodal line directed offshore just north of the canyon that separates the two regions of maximum variability. The spatial distribution of integrated PSD centered at 52.7 cpd (27.3 min) closely resembles the modal pattern shown in Fig. A2d, which corresponds to the fourth mode of oscillation with a period of 23.3 min. We also infer the existence of two nodal lines that are directed offshore from the coast in each half of the bay that are located almost exactly where they are predicted to occur in Fig. A2d. At a center frequency of 66.9 cpd (21.5 min), Fig. 11d shows an even more complex and highly localized modal pattern that resembles the fifth mode of oscillation predicted by WHK (not shown). These spatial patterns obtained from the power spectra are particularly helpful in allowing us to see how the modal patterns are related to specific frequencies. The agreement between the spatial patterns obtained from ROMS and those from WHK, is excellent in at least two cases, at 26.0 cpd and at 52.7 cpd. There is less agreement in the predicted periods, however.

Three additional model simulations have been performed to search for the mechanism or mechanisms responsible for exciting the natural oscillations of Monterey Bay. The first simulation employs observed hourly wind forcing without tidal forcing. The second simulation employs constant wind forcing. In this case, the wind stress at each model grid point is the averaged wind stress over the whole model domain at that time step. Thus, the wind stress is constant in space and changes only with time. The third simulation employs uniform wind forcing. The wind stress in this experiment is the time average of the wind stress used in the second experiment, and thus does not change in space or time. The integrated PSD for the frequency band 24–28 cpd at the closest

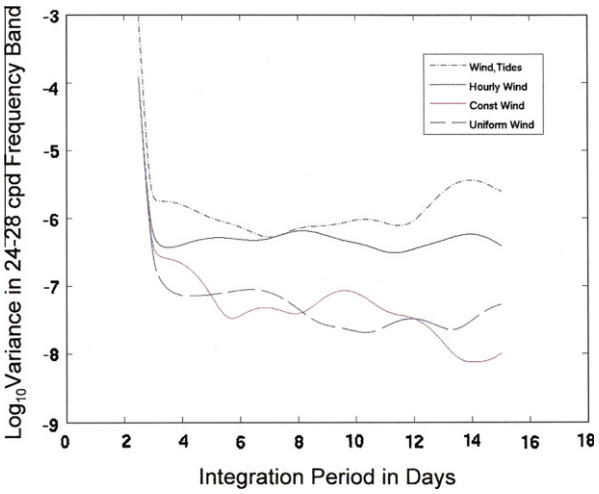

Fig. 12. Time evolution of integrated power spectra of sea surface height for the frequency band 24–28 cpd for the ROMS model grid point nearest Monterey. The power spectra are computed using 6-min sea surface height model output for each 5-day window. The results for four simulations are shown: with tides and hourly wind stress forcing (dash-black), with hourly wind stress forcing only (black), constant wind stress forcing only (red), and uniform wind stress forcing only (blue). The vertical axis represents the variance in this frequency band on a logarithmic scale. The horizontal axis represents the number of days of model integration. In the case of constant wind stress forcing, the wind stress does not change in space. For the case of uniform wind stress forcing, the wind stress does not change in space or time. (For interpretation of the references to colour in this figure legend, the reader is referred to the web version of this article.)

model point to Monterey is shown in Fig. 12. The PSDs are calculated using 6-min model output with a moving window of 5 days. From this figure, it is clear that steady state conditions are reached after approximately 3 days of model spin up in each case. The model integration with both tidal and hourly wind forcing produced the highest levels of variance in the 24–28 cpd frequency band. Removing tidal forcing reduces the level of variance of this frequency band by roughly half an order-of-magnitude. With constant or uniform wind stress forcing, the variance is further reduced by one order-of-magnitude. We find these results illuminating since they suggest that both the natural variability associated with the observed winds, and tidal forcing most likely contribute to the natural oscillations in Monterey Bay, but that wind forcing may contribute to a greater extent than tidal forcing. However, it should be noted that these model results apply only to the Monterey Bay region, and so other factors such as long-period surface waves that originate far offshore are not taken into account.

4. Possible mechanisms for exciting the natural oscillations of Monterey Bay

As shown in Section 2, and in Breaker et al. (2008), the natural oscillations of Monterey Bay are not transient, as might be expected, but are essentially continuous functions of time. We find the continuous nature of these oscillations curious, and, as a result, have probed this question a bit further. The numerical simulations above support the general view that the winds and tides may contribute to the natural oscillations in Monterey Bay. However, these mechanisms do not tell us what the actual linkage(s) is between these forcing functions and the oscillations per se. Here, we consider several processes that could provide this linkage.

Initially, we considered four possible mechanisms that could provide the link between the forcing and the bay's response. One possibility is that the oscillations in Monterey Bay are excited by edge waves. According to Lemon (1975) and LeBlond and Mysak (1978), edge waves traveling along the coast of Vancouver Island impinge on the entrance of San Juan Bay and excite the natural modes of oscillation within the bay. Recent measurements in Monterey Bay in the infragravity wave frequency band by MacMahan et al. (2004a), and MacMahan et al. (2004b) showed that within the infragravity band, highly energetic rip currents, surf zone eddies, and presumably, edge waves occur. Thus, edge waves could serve as a source of excitation for the oscillations in Monterey Bay. Edge waves are related to incoming surface gravity waves that are related to local and remote wind forcing, both of which vary significantly on short times scales (days to weeks) and seasonally, as well. Thus, the presence of edge waves is time dependent and so is not necessarily consistent with the continuous oscillations in Monterey Bay.

It is also possible that long-period surface waves produced by low-frequency oscillations in the atmosphere that originate far offshore, subsequently enter the bay producing surges in water level that lead to seiching (Wilson, 1956; WHK). We note that this explanation is consistent with our own findings regarding the likely importance of offshore forcing, but inconsistent in that such forcing would be expected to be seasonal and so are not generally consistent with our results.

Another possible mechanism for producing seiching on a regular basis is that surges are generated next to the coast due to the vigorous sea breeze circulation that occurs in Monterey Bay (e.g., Banta et al., 1993; Round, 1993). The sea breeze is strongest between May and August. O'Connor (1964) examined sea level anomalies from tide gauge measurements in Monterey Harbor and found that the largest anomalies were due to the sea breeze circulation in Monterey Bay, producing sea level departures as large as 25–30 cm. The diurnal nature of the surge could produce seiche oscillations on a regular basis. Again, if this mechanism does, in fact, contribute to seiche oscillations within the bay, a seasonal pattern would be expected since the sea breeze circulation is far stronger during the summer.

With respect to tidal forcing, it is possible that breaking internal waves in and around MSC produce internal pressure fluctuations that could serve as a source of excitation for the natural oscillations of Monterey Bay. According to Carter and Gregg (2002), intense mixing takes place near the head of MSC, with turbulent kinetic energy up to 1000 times greater than in the open ocean. According to the results of Key (1999), the internal tide in MSC was found to be highly nonlinear and bottom currents and temperatures often revealed the characteristics of an internal tidal bore, which could in turn lead to internal wave breaking. Relevant to this study, Key also found that the formation of bores did not occur on a continuous or periodic basis but rather tended to occur intermittently. Finally, to our knowledge, observations of internal wave breaking per se have yet to be reported.

Two additional mechanisms have also been considered as possible sources of the natural oscillations in Monterey Bay, small-scale turbulence and ocean microseisms. Because small-scale turbulence is characteristically intermittent in nature we do not believe that this mechanism is ultimately responsible for these oscillations (personal communication, E. Kunze). Although ocean microseisms, because of their ubiquitous nature, are appealing as a possible source of continuous excitation, the energy associated with them at frequencies below 0.10 cycles per second decreases rapidly and thus may be negligible at the frequencies of interest (personal communication, S. Webb).

None, one, or several of the mechanisms that have been considered could be responsible for the continuous nature of the oscillations we have observed in Monterey Bay. Although a detailed search of the literature has not revealed similar observations in other closed or semi-enclosed basins, we believe that this is most

likely due to at least two factors: first, the amplitudes of these oscillations are relatively small and so could easily be missed in any cursory examination of the available data, and second, there has been no obvious reason to search for them. However, we find it hard to believe that such oscillations occur only in Monterey Bay and so a mechanism that is global in extent would be high on our list of possibilities. If we are correct, this adds significantly to the generality of our results.

5. Discussion and conclusions

The natural oscillations of Monterey Bay have been examined on a number of occasions, with results that sometimes appear contradictory. On the observational side, different methods of data collection, record lengths, and methods of analysis have undoubtedly contributed to some of these differences. Also, as demonstrated in Fig. 4a and b, the signals of interest are weak and not well resolved, making it more difficult to estimate their exact frequencies. In the present study, and in a recent study by Breaker et al. (2008), four frequencies with periods in the vicinity of 55, 37, 27 and 22 min were consistently observed at Monterey, in Elkhorn Slough, and at Santa Cruz. The 55-min period most likely corresponds to the first longitudinal mode of oscillation and the 37-min period to the first transverse mode, based on the dimensions of the bay and the results of WHK. The existence of a natural oscillation with a period of 37 min was further demonstrated by a frequency analysis of the sea level response to the Great Alaskan Earthquake of 1964. Many higher frequency oscillations have also been observed or predicted. However, these higher frequency oscillations may be harmonically related to the lower frequencies or may not be bay-wide in their extent.

The model results of WHK indicate that the MSC has a significant effect on the oscillating system, where the canyon essentially separates the bay into two semi-independent halves with only weak coupling between them. Results from a numerical model employed in this study also suggest that MSC plays a role in separating oscillating regimes to the north and south of the canyon. Although the canyon may serve as a barrier for the higher frequency oscillations, our observations, and those of Raines (1967), Robinson (1969), and Lynch (1970) suggest that this is not the case, at least for the four lowest frequencies.

Significant differences were often found in the results of WHK between their observations and model predictions for the primary periods of oscillation in Monterey Bay. In the models they employed, a nodal line was always assumed to lie across the mouth of the bay from Pt. Piños, on the Monterey Peninsula, to Pt. Santa Cruz, at the north end of the bay. WHK acknowledged that this assumed location for the nodal line could be incorrect and thus might account for some of the discrepancies in their results. Results from this study suggest that such a nodal line could be located up to 10 km further offshore. Our results further show that by extending the nodal line only 5 km further offshore, much better agreement between observations and theory is obtained.

To gain more insight into the nature of these oscillations, we employed two state-of-the-art hydrodynamic circulation models to examine the effects of both impulsive and realistic wind forcing on the resonant characteristics of the bay. The impulsive wind forcing was applied for a specified period for various wind directions around the bay. Maximum amplitudes, number of oscillations, and the mean periods of the oscillations were obtained from the model simulations. Wind forcing from the west and northwest generally produced maximum amplitudes and the largest number of oscillations. Winds from the north, northwest, and south produced periods in the range of 50–60 min, consistent with the first longitudinal mode of oscillation for the bay.

Based on a quality factor analysis of the data and model simulations, we expect impulsively generated seiche oscillations in Monterey Bay to decay within roughly 3–6 cycles. However, one characteristic that we found intriguing about these oscillations is their continuous nature, since seiche oscillations are generally transient due to the transient nature of the forcing. Our observations show rather clearly the continuous nature of the four lowest frequency oscillations. We have shown that weather events, particularly during the winter, do excite these oscillations, as they should, but the mechanism that is responsible for maintaining them when obvious transient disturbances are not present must be due to another mechanism that provides continuous forcing. Six mechanisms were considered as possible sources for these continuous oscillations, but it s not clear which, if any, of these mechanisms is ultimately responsible for exciting them. However, it is difficult to conceive that such oscillations occur only in Monterey Bay, and, if it turns out that the excitation is global in nature, then our results may apply to other resonant basins around the world as well.

Acknowledgments

The authors would especially like to thank Jerrold Norton for providing the tidal records from Monterey that were used in our analysis of the Loma Prieta and Great Alaskan earthquakes. He also provided considerable background information regarding the data and how it was collected. We also thank Dustin Carroll who painstakingly digitized both records. Dr. Raphael Kudela and Brian Hoover are thanked for providing the pressure data from the Santa Cruz wharf. The first author would like to thank Joan Parker for conducting a survey of publications on seiches in the oceanographic literature showing how the interest in this subject grew and peaked toward the middle of the last century due most likely to the fact that analytic solutions to the governing equations could often be found. Dr. T.S. Murty and Dr. Edward Thornton are thanked for reviewing earlier versions of the manuscript and for making a number of helpful comments. Finally, Dr. Eric Kunze and Dr. Spahr Webb are thanked for helpful discussions on clarifying the possible role of small-scale turbulence and ocean microseisms, respectively, in contributing to the continuous nature of the natural oscillations of Monterey Bay.

Appendix A. Theoretical normal modes of oscillation for Monterey Bay

WHK examined the three-dimensional (3D) modes of oscillation for Monterey Bay using Stoker's numerical solutions to the governing equations. Following Stoker's method, determining the 3D oscillations in lakes and bays is an eigenvalue problem that can be solved using linearized long-wave theory together with finite differences. The bay was modeled using a polar coordinate network of grid points. WHK considered the results they obtained using Stoker's method of numerical solution to be the most accurate. Fig. A1 shows the normalized modal pattern for the first mode 3D oscillation that was obtained from the numerical calculations. The contours represent water level elevations above (+), or below (−), still water, normalized to unit value at the highest antinode. The small inset in the lower left-hand corner shows the type of oscillation that occurs. Of importance is the nodal line that is shown across the entrance of the bay because the model results are based on a nodal line at this location. As indicated, the first mode has a predicted period of 44.2 min, and the oscillating pattern is confined to the northern half of the bay, apparently isolated from the southern half of the bay by the presence of the MSC.

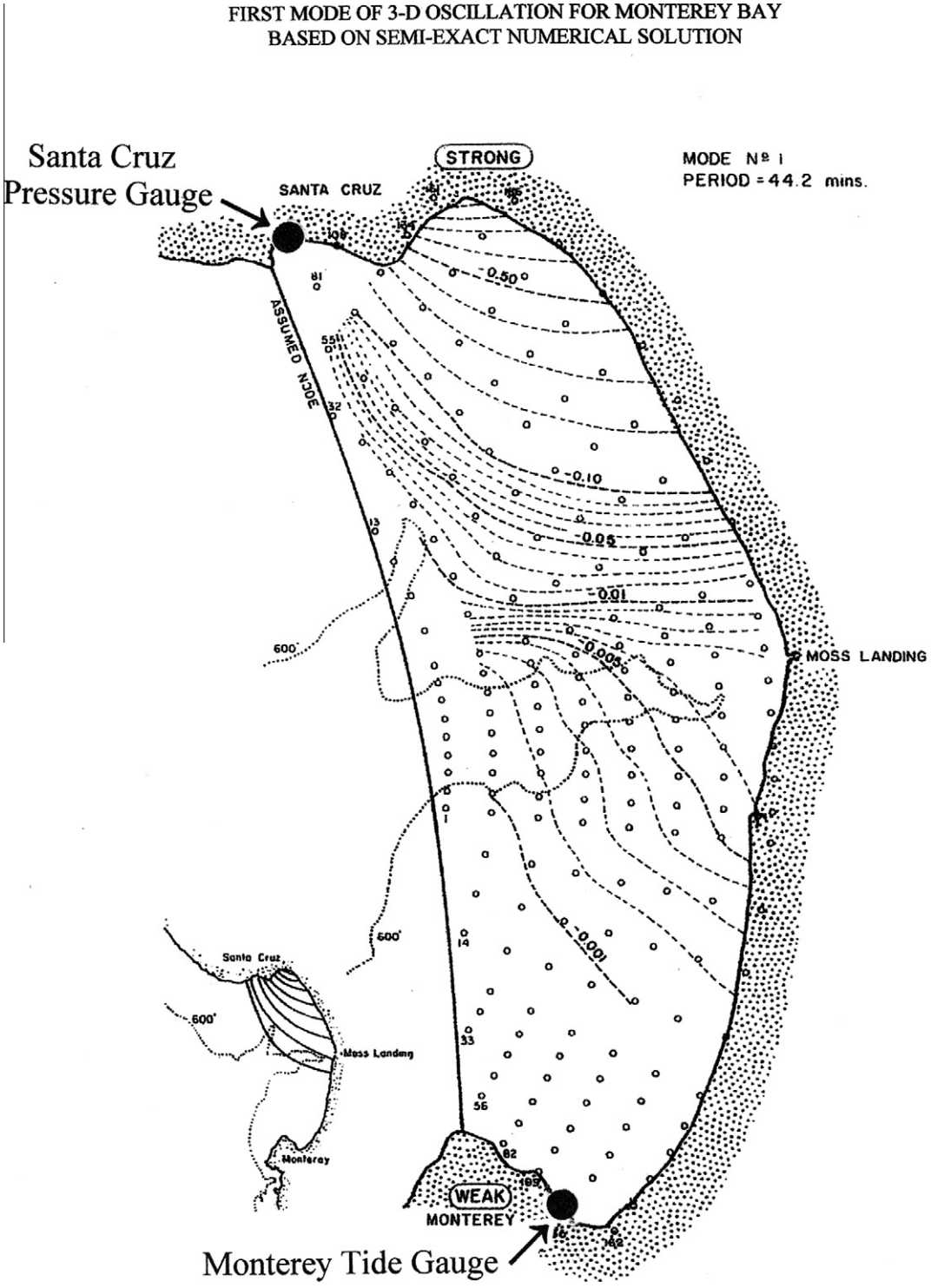

Fig. A1. The spatial pattern for the first three-dimensional mode of oscillation for Monterey Bay, based on a semi-exact numerical solution (see WHK for details). Water level elevations above or below still water (dashed lines) are scaled according to the maxima which occur at the antinodes, and the depths are expressed in feet (dotted lines). The inset in the lower-left-hand corner shows a simplified version of the type of oscillations that occur. The locations where the water level data in Monterey Harbor and the pressure data at Santa Cruz were acquired are shown by the two large black dots at each end of the bay.

Fig. A2 shows the insets for modes 1–4. The first mode was shown in Fig. A1. The second mode has a period of 29.6 min and is again confined to the northern half of the bay, although its oscillating pattern shows two antinodes rather than one, as indicated in Fig. A2b. The third mode has a period of 28.2 min, is confined to the southern half of Monterey Bay, and has one antinode located in Monterey Harbor (Fig. A2c). The fourth mode has a period of 23.3 min (Fig. A2d), and spans the entire bay, having antinodes located at each end, and a third antinode located at the center of the bay near Moss Landing. Modes up to 22 were calculated and generally the patterns become more complicated and localized and the amplitudes become smaller, and so

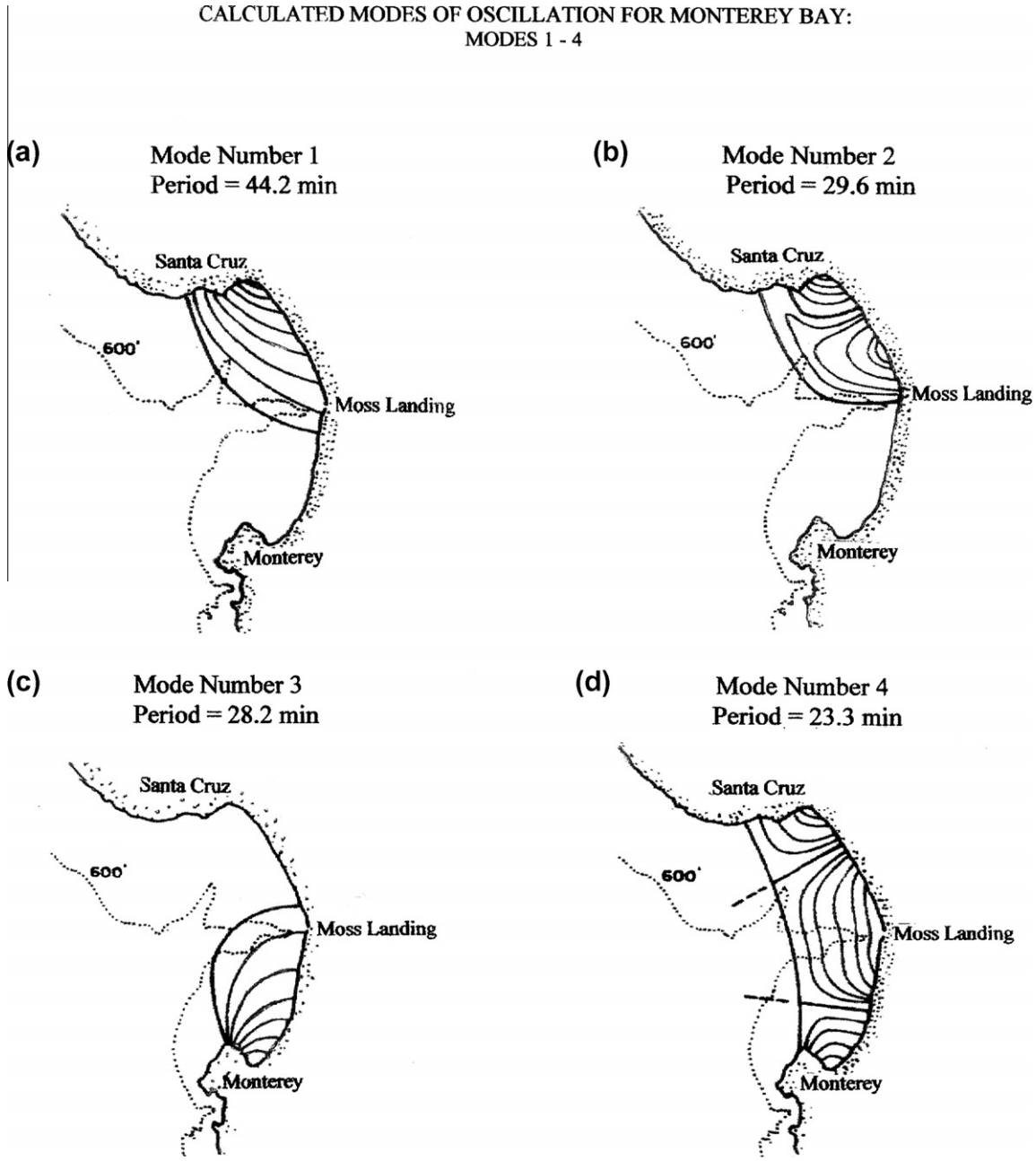

Fig. A2. Modal patterns for the first four modes of oscillation for Monterey Bay from WHK: (a) the first mode, (b) the second mode, (c) the third mode, and (d), the fourth mode. The corresponding predicted periods for these modes are 44.2, 29.6, 28.2, and 23.3 min, respectively.

we expect the influence of the higher modes to decrease accordingly.

References

Banta, R.M., Olivier, L.D., Levinson, D.H., 1993. Evolution of the Monterey sea-breeze layer as observed by pulsed doppler Lidar. Journal of Atmospheric Sciences 50, 3959–3982.

Breaker, L.C., Broenkow, W.W., 1994. The circulation of Monterey Bay and related processes. Oceanography and Marine Biology: An Annual Review 32, 1–64.

Breaker, L.C., Broenkow, W.W., Watson, W.E., Jo, Y.-H., 2008. Tidal and non-tidal oscillations in Elkhorn Slough, California. Estuaries and Coasts 31, 239–257.

Breaker, L.C., Murty, T.S., Norton, J.G., Carroll, D., 2009. Comparing the sea level response at Monterey, California to the Loma Prieta Earthquake of 1989 and the Great Alaskan Earthquake of 1964. Science of Tsunami Hazards 28, 255–271.

Carter, G.S., Gregg, M.C., 2002. Intense, variable mixing near the head of Monterey Submarine Canyon. Journal of Physical Oceanography 32, 3145–3165.

Crowell, B., <http://creativecommons.org/licesnses/by-sa/1.0/>, 2006. Vibrations and Waves. Licensed under the Creative Commons Attribution-Share-Alike License, Version 1.0. ISBN:0-9704670-3-6.

Defant, A., 1961. Physical Oceanography, vol. II. The MacMillan Company, New York.

Dietrich, D.E., Lin, C.A., 2002. Effects of the hydrostatic approximation and resolution on the simulation of convective adjustment. Tellus, Series A 54, 34–43.

Egbert, G.D., Erofeeva, S.Y., 2002. Efficient inverse modeling of barotropic ocean tides. Journal of Atmospheric and Oceanic Technology 19, 183–204.

Egbert, G.D., Bennett, A.F., Foreman, M.G., 1994. TOPEX/POSEIDON tides estimated using a global inverse model. Journal of Geophysical Research 99, 24821–24852.

Flather, R.A., 1976. A tidal model of the north-west European continental shelf. Memoirs of the Royal Society of Sciences of Liege 6, 141–164.

Giese, G.S., Chapman, D.C., Black, P.G., Fornshell, J.A., 1990. Causation of large-amplitude coastal seiches on the Caribbean coast of Puerto Rico. Journal of Physical Oceanography 20, 1449–1458.

Golyandina, N., Nekrutkin, V., Zhigljavsky, A., 2001. Analysis of Time Series Structure: SSA and Related Techniques. Monographs on Statistics and Applied Probability, vol. 90. Chapman&Hall/RC, Boca Raton.

Haney, R.L., Hale, R.A., Dietrich, D.E., 2001. Offshore propagation of eddy kinetic energy in the California Current. Journal of Geophysical Research 106, 11709–11717.
Hodur, R.M., 1997. The Naval Research Laboratory's Coupled Ocean/Atmosphere Mesoscale Prediction System (COAMPS). Monthly Weather Review 125, 1414–1430.
Honda, K., Isitani, D., Terada, T., Yoshida, I., 1908. An investigation of the secondary undulations of oceanic tides. Journal of the Faculty of Science 24, 1–113.
Hough, S.S., 1898. On the application of harmonic analysis to the dynamical theory of tides. Part II. On the general integration of LaPlace's dynamical equations. Philosophical Transactions of the Royal Society of London Series A 191, 138–185.
Jackson, J.D., 1962. Classical Electrodynamics. John Wiley & Sons, Inc., New York.
Key, S.A., 1999. Internal Tidal Bores in the Monterey Canyon. M.S. Thesis, Naval Postgraduate School, Monterey, California.
Kondo, J., 1975. Air–sea bulk transfer coefficients in diabatic conditions. Boundary Layer Meteorology 9, 91–112.
Kowalik, Z., Murty, T.S., 1993. Numerical Modeling of Ocean Dynamics. World Scientific, Singapore.
LaPlace, P.S., 1775. Researches sur plusiers points du systeme du monde. Memoires de l'Academie Royale des Sciences 88, 75–182.
Large, W.G., McWilliams, J.C., Doney, S.C., 1994. Oceanic vertical mixing: a review and a model with non-local boundary layer parameterization. Reviews of Geophysics 32, 363–403.
LeBlond, P.H., Mysak, L.A., 1978. Waves in the Ocean. Elsevier Scientific Publishing Company, Amsterdam.
Lemon, D.D., 1975. Observations and Theory of Seiche Motions in San Juan Harbor, B.C. M.S. Thesis, The University of British Columbia, 81 pp.
Lynch, T.J., 1970. Long Wave Study of Monterey Bay. M.S. Thesis, Naval Postgraduate School, Monterey, California.
Ma, K., Sataki, K., Kanamori, H., 1990. Tsunami of the 1989 Loma Prieta Earthquake. EOS Transactions 71, pp. 1460 (abstract).
MacMahan, J.H., Reniers, Ad.J.H.M., Thornton, E.B., Stanton, T.P., 2004a. Infragravity rip current pulsations. Journal of Geophysical Research 109, C01033. doi:10.1029/2003JC002068.
MacMahan, J.H., Reniers, Ad.J.H.M., Thornton, E.B., Stanton, T.P., 2004b. Surf zone eddies coupled with rip current morphology. Journal of Geophysical Research 109, C07004. doi:10.1029/2003JC002083.
Malloy, R.J., 1964. Crustal uplift southwest of Montague Island, Alaska. Science 146, 1048–1049.
Marchesiello, P., McWilliams, J.C., Shchepetkin, A., 2001. Open boundary condition for long-term integration of regional oceanic models. Ocean Modelling 3, 1–21.
McNutt, S., 1990. Loma Prieta Earthquake, October 17, 1989. California Geology 43, 3–7.
Murty, T.S., 1977. Seismic Sea Waves – Tsunamis. Bull. Fish. Res. Board Canada 198, Ottawa.
Neumann, G., Pierson, W.J., 1966. Principles of Physical Oceanography. Prentice-Hall Inc., Englewood Cliffs, New Jersey.
O'Connor, P., 1964. Short-term Sea Level Anomalies at Monterey, California. M.S. Thesis, Naval Postgraduate School, Monterey, California.
Okihiro, M., Guza, R.T., 1996. Observations of seiche forcing and amplification in small harbors. Journal of Waterway, Port, Coastal, and Ocean Engineering 122, 232–238.
Pacanowski, R.C., Philander, S.G.H., 1981. Parameterization of vertical mixing in numerical models of tropical oceans. Journal of Physical Oceanography 11, 1443–1451.
Page, R., 1968. Aftershocks and microaftershocks of the great Alaska earthquake of 1964. Bulletin of the Seismological Society of America 58, 1131–1168.
Parks, T.W., Burrus, C.S., 1987. Digital Filter Design. John Wiley & Sons, New York.
Raines, W.A., 1967. Sub-tidal Oscillations in Monterey Harbor. M.S. Thesis, Naval Postgraduate School, Monterey, California.
Robinson, D.B., 1969. Seiching in Monterey Bay. M.S. Thesis, Naval Postgraduate School, Monterey, California.
Round, RT.D., 1993. Climatology and Analysis of the Monterey Bay Sea Breeze. M.S. Thesis, Naval Postgraduate School, Monterey, California.
Schepetkin, A., McWilliams, J.C., 2005. The Regional Oceanic Modeling System (ROMS): a split-explicit, free-surface, topography-following-coordinate ocean model. Ocean Modelling 9, 347–404.
Schwing, F.B., Norton, J.C., Pilskaln, C.H., 1990. Earthquake and Bay: Response of Monterey Bay to the Loma Prieta Earthquake. EOS, Transactions of the American Geophysical Union: The Oceanography Report, 71, 4 pp.
Sobey, R.J., 2006. Normal mode decomposition for identification of storm tide and tsunami hazard. Coastal Engineering 53, 289–301.
Song, Y.T., Haidvogel, D., 1994. A semi-implicit ocean circulation model using a generalized topography-following coordinate system. Journal of Computational Physics 115, 228–244.
Stoker, J.J., 1957. Water Waves. Interscience Publishers, Inc., New York.
Thompson, D.J., 1982. Spectrum estimation and harmonic analysis. IEEE Proceedings 70, 1055–1096.
Thompson, D.J., 1990. Quadratic-inverse spectrum estimates: applications to paleoclimatology. Philosophical Transactions of the Royal Society of London, Series A 332A, 539–597.
Tseng, Y.-H., 2003. On the Development of a Ghost-cell Immersed Boundary Method and its Application to Large Eddy Simulation and Geophysical Fluid Dynamics. Ph.D. Thesis, Stanford University, Stanford, California.
Tseng, Y.-H., Breaker, L.C., 2007. Non-hydrostatic simulations of the regional circulation in the Monterey Bay area. Journal of Geophysical Research 112, C12017. doi:10.1029/2007JC004093.
Tseng, Y.-H., Ferziger, J.H., 2003. A ghost-cell immersed boundary method for flow in complex geometry. Journal of Computational Physics 192, 593–623.
Tseng, Y.-H., Ferziger, J.H., <http://www.informaworld.com/smpp/content~content=a744411426~db=all>, 2004. Large-eddy simulation of turbulent wavy boundary flow: illustration of vortex dynamics. Journal of Turbulence 5.
Tseng, Y.-H., Dietrich, D.E., Ferziger, J.H., 2005. Regional circulation of the Monterey Bay region: hydrostatic versus non-hydrostatic modeling. Journal of Geophysical Research 110, C09015. doi:10.1029/203JC002153.
Tukey, J.W., 1961. Discussion, emphasizing the connection between analysis of variance and spectrum analysis. Technometrics 3, 191–219.
Wang, X., Chao, Y., Dong, J., Farrara, Z., Li, Z., McWilliams, J.C., Paduan, J.D., Rosenfeld, L.R., 2009. Modeling the tides in Monterey Bay, California. Deep-Sea Research II 56, 219–231.
Weedon, G.P., 2003. Time-Series Analysis and Cyclostratigraphy. Cambridge University Press, Cambridge.
Welch, P.D., 1967. The use of the Fast Fourier Transform for the estimation of power spectra: a method based on time averaging over short, modified periodograms. IEEE Transactions on Audio and Electroacoustics AU-15, 70–73.
Wilson, B.W., 1956. The Origins and Effects of Long-period Waves in Ports. A&M Project 24, Reference 56-20T, The Agricultural and Mechanical College of Texas, 36 pp.
Wilson, B.W., 1972. Seiches. Advances in Hydroscience 8, 1–94.
Wilson, B.W., Hendrickson, J.A., Kilmer, R.E., 1965. Feasibility Study for a Surge-action Model of Monterey, California. US Army Corps of Engineers, Waterways Experiment Station, Vicksburg, MS. 166 pp.
Wong, F.L., Eittreim, S.E., 2001. Continental Shelf GIS for the Monterey Bay National Marine Sanctuary. US Geological Survey Open File Report, 179 pp.